Drug and Chemical Toxicology

ISSN: 0148-0545 (Print) 1525-6014 (Online) Journal homepage: http://www.tandfonline.com/loi/idct20

Lead induces Siberian tiger fibroblast apoptosis by interfering with intracellular homeostasis

Zheng Liu, Hui Wang, Wenxiu Zhang, Ziao Yuan, Hongyi Yuan, Xueting Liu, Minghai Zhang, Xuesong Guo & Weijun Guan

To cite this article: Zheng Liu, Hui Wang, Wenxiu Zhang, Ziao Yuan, Hongyi Yuan, Xueting Liu, Minghai Zhang, Xuesong Guo & Weijun Guan (2017): Lead induces Siberian tiger fibroblast apoptosis by interfering with intracellular homeostasis, Drug and Chemical Toxicology, DOI: 10.1080/01480545.2017.1337125

To link to this article: http://dx.doi.org/10.1080/01480545.2017.1337125

Published online: 21 Jun 2017.

DRUG AND CHEMICAL TOXICOLOGY, 2017
https://doi.org/10.1080/01480545.2017.1337125

Taylor & Francis
Taylor & Francis Group

RESEARCH ARTICLE

Lead induces Siberian tiger fibroblast apoptosis by interfering with intracellular homeostasis

Zheng Liu[a], Hui Wang[a], Wenxiu Zhang[b], Ziao Yuan[b], Hongyi Yuan[b], Xueting Liu[b], Minghai Zhang[c], Xuesong Guo[a] and Weijun Guan[b]

[a]College of Food Science and Engineering, Jinzhou Medical University, Jinzhou, Liaoning, China; [b]Institute of Animal Science, Chinese Academy of Agricultural Sciences, Beijing, China; [c]College of Wildlife Resources, Northeast Forestry University, Harbin, Heilongjiang, China

ABSTRACT

Lead (Pb^{2+}) is a poisonous heavy metal that causes many pathophysiological effects in living systems. Its toxicological effects are well known as it causes apoptosis of several cell types and tissues. This study aimed to determine the criteria required for early diagnosis of Pb^{2+} poisoning in the Siberian tiger using a tiger population in China, to identify a safety Pb^{2+} concentration threshold, and to provide suggestions for preventing Pb^{2+} poisoning in Siberian tigers. We investigated the apoptotic effects of Pb^{2+} (0, 32, 64, and 125 μM) for 12–48 h on Siberian tiger fibroblasts *in vitro*. Typical apoptotic effects were observed after Pb^{2+} exposure. Pb^{2+} strongly blocked DNA synthesis in the G0/G1 phase and induced cell apoptosis in a dose- and time-dependent manner. Intracellular free calcium (Ca^{2+}) levels, reactive oxygen species levels, and efflux of extracellular Ca^{2+} were increased. The mitochondrial membrane potential was lowered. Caspase-3, -8, and -9 activities were increased when fibroblasts were treated with 32, 64, and 125 μM Pb^{2+}. The gene expression levels of Bax, caspase-3, -8, Fas, and p53 were increased, while that of Bcl-2 was decreased. Calcium homeostasis and mitochondrial function were disturbed. Ca^{2+} efflux, oxidative damage, activation of caspases, and regulation of Bax, Bcl-2, caspase-3, -8, Fas, and p53 gene expression played an important role in the apoptotic effects. The disorder of intracellular homeostasis was the trigger for apoptosis in Siberian tiger fibroblasts.

ARTICLE HISTORY
Received 12 May 2016
Revised 5 May 2017
Accepted 28 May 2017

KEYWORDS
Siberian tiger; lead; apoptosis; fibroblasts

Introduction

The Siberian tiger, the largest tiger subspecies, has a reputation of being the king of the forest in the world. Currently, the wild population is mainly distributed in northeast China, Russian Far East, and northern Korea (Matyushkin *et al.* 1999). In China, the Siberian tiger is widely distributed in the forest of northeastern region. However, because of poaching and environmental deterioration, there has been a sharp drop in the number of the wild populations. The distribution has gradually reduced, thus making it one of the world's most endangered big cat. Habitat destruction is the main reason for its decline and distribution reduction (Miquelle and Pikunov 2003). Heavy metal accumulation and pollution in the forest ecosystems has not only destroyed the tiger habitats but also destroyed the tiger's food sources such as hoofed animals, roe deer, wild boar, and red deer (Russello *et al.* 2004). With the rapid development of modern industries, agriculture, and transportation, the tiger habitat is under serious threat, especially in areas with heavy metal pollution. This has led to a significant impact on the Siberian tiger's growth, development, and disease incidence.

Lead is a natural environmental and potentially carcinogenic poisonous heavy metal, which has been widely dispersed in the environment and remains in the biotope. Lead is a common heavy metal pollutant and a byproduct of many artificial sources that is released into the environment. Lead pollution mainly originates from all kinds of industrial production such as batteries, chemicals, gasoline, pesticide, paint, dyes, and various kinds of metal production. For Siberian tigers, the major sources of exposure to lead compounds include air, dust, food, and water (Yin and Huang 1999). Lead is an important element in environmental toxicology studies. Lead causes many pathophysiological effects in living systems such as neurotoxicity, reproductive toxicity, kidney damage, liver toxicity, hematological dysfunctions, and immunotoxicity (Mielke and Reagan 1998). Lead has shown to cause kidney, brain, and lung cancers in experimental rodents (IARC 1987, Gerber *et al.* 1980, Goyer 1993). Further, research on experimental animals exposed to low levels of lead has shown significant adverse outcomes such as chronic kidney disease, high blood pressure, and resistance index (Roncal *et al.* 2007, Villeda-Hernandez *et al.* 2006). It could also affect many kinds of cells, and induce oxidative stress and dysfunction in many cell types (Srianujata 1998). Lead exposure can result in gene mutations in many cultured cells (Zelikoff *et al.* 1988, Roy and Rossman 1992, Ariza and Williams 1996, Yang *et al.* 1996). Lead can induce

CONTACT Xuesong Guo guoxuesongly@163.com Jinzhou Medical University, Jinzhou 121001, China; Weijun Guan guanweijun@outlook.com Institute of Animal Science, Chinese Academy of Agricultural Sciences, Beijing 100193, China

degeneration and atrophy of the testicular cells, denature reproductive cells, block the reproductive process, and decrease the sperm number (Dong *et al.* 2005). Exposure to lead is detrimental to the central nervous system and learning abilities. Low levels of lead exposure could also result in neurotoxic effects (Dominguez *et al.* 2002).

Lead poisoning is a concern in some countries wherein there is use of leaded gasoline, hyperurbanization, and industrial pollution (Kwong *et al.* 2004). Forest ecosystem pollution has become an important global environmental concern. Heavy metal pollution leads to the forest ecological deterioration and serious damage to the virtuous cycle of the forest ecosystem and wildlife habitat. In the ecological environment, tiger is at the top of the food chain, and it plays a key role in the ecosystem. Tiger is not only an important species for biodiversity conservation, but is also considered as an indicator species of an intact ecosystem. Protection of wild Siberian tiger helps in protecting other wild animals and natural ecosystem, which are closely related to humans. The toxic effect and mechanism of lead effects on Siberian tigers have not yet been elucidated. The aims of this study were to examine the effects of lead-induced apoptosis in Siberian tiger fibroblasts and to investigate the cellular and molecular mechanisms by which lead causes apoptosis in the fibroblasts, determine the safety threshold limits, and provide a scientific basis for the lead poisoning protection of the Siberian tiger.

Materials and methods

Materials

A Siberian tiger fibroblast cell line derived from Siberian tiger ear marginal tissue and passaged three times was provided by the Institute of Animal Science, Chinese Academy of Agricultural Sciences. The fibroblasts were authenticated by the supplier and tested negative for contaminations. Propidium iodide (PI) and lead acetate ($Pb(Ac)_2$, purity, 99.999%) were purchased from Sigma (St. Louis, MO). Dulbecco's modified Eagle's medium (DMEM) and fetal bovine serum (FBS) were purchased from Gibco (Grand Island, NY). Annexin V-FITC Apoptosis Detection Kit I was purchased from Becton Dickinson Company (Franklin Lakes, NJ).

Cell culture

The cells were cultured in DMEM that was supplemented with 10% FBS and incubated under 5% CO_2 and 95% air at 37 °C and saturation humidity. The medium was changed when it turned yellow. When the cells reached 80–90% confluence, they were digested and passaged.

Drug solution preparation and cell treatment

Lead acetate was dissolved in DMEM, filtered through a 0.22-μm filter, and aliquoted. Lead was diluted to the required concentration with DMEM before usage. The experimental cells in the logarithmic phase were treated with a range of Pb^{2+} concentrations (0, 32, 64, or 125 μM) at scheduled times.

Hoechst 33258 staining

Sterilized coverslips were placed inside the culture plate. Cells were allowed to grow on the cover slips. When the cells entered the logarithmic growth phase, Pb^{2+} was added for treatment for 24 h, after which a fixative was added. Subsequently, the cells were washed, after which Hoechst 33258 staining solution was added. Antifade mounting medium was added to the stained cells on the slides after which coverslips were used to avoid the air bubbles. Then, the cells were observed and photographed using confocal microscopy (Nikon TE-2000-E, Tokyo, Japan).

Transmission electron microscopy (TEM)

Control and experimental cells were fixed with 2.5% glutaraldehyde. The cells were further fixed with 1% osmium tetroxide and rinsed with 0.1 M phosphate buffer. Dehydration was carried out in a graded series of acetone (30%, 50%, 70%, 80%, 90%, and 100%). The cultures were embedded on SPURR discs in epoxy resin for polymerization. LEICAUC6i ultrathin microtome was used for cutting sections, which were stained with uranyl acetate and lead citrate. The cells were then photographed by TEM (JEM-2000Ex; JEOL Ltd., Tokyo, Japan).

Annexin V-FITC/PI double labeling

Cells were treated with Pb^{2+} for 12, 24, 36, and 48 h. The cell concentrations in the control and experimental groups were adjusted to 4.0×10^5 cells/ml with binding buffer. In each sample of 100-μL cell suspension, 5 μL of fluorescein isothiocyanate (FITC) and 5 μL of PI were added and incubated for 15 min. Then, 400 μL of binding buffer was added into each sample, and the cells were analyzed by flow cytometry (FC500, Beckman Coulter, Brea, CA). At least 10 000 cells were analyzed for each sample.

Cell cycle analysis

Prechilled 70% ethanol was added to the control and experimental group cells (4.0×10^5 cells/mL) and incubated at 4 °C overnight. Thereafter, the cells were washed with PBS, incubated with 0.02 mg/mL RNase A, and stained with PI solution (PI, 0.05 mg/ml; sodium citrate, 1 mg/mL; NaCl, 0.585 g/ml, pH 7.2–7.6) for 20 min. Then, the cells were analyzed by flow cytometry (FC500, Beckman Coulter). At least 10 000 cells were analyzed for each sample.

Mitochondrial membrane potential

Control and experimental groups cells were collected after adjusting the cell concentration of 4.0×10^5 cells/mL; 0.5 mL of JC-1 (5,5′, 6,6′-tetrachloro-1,1′,3,3′-tetraethylbenzimidazolcarbocyanine iodide) staining solution (5 μg/mL, 0.5 mL/sample) was added and then the cells were incubated in a CO_2 incubator in the dark for 15 min. Next, the cells were washed twice with pre-warmed PBS. The supernatant was discarded by centrifugation, and then, 0.5 mL PBS was added to

each sample. Thereafter, the cells were analyzed by flow cytometry (FC500, Beckman Coulter). At least 10 000 cells were determined for each sample.

Intracellular Ca^{2+} homeostasis

Fluo-3/Am was dissolved in DMSO at a final concentration of 2 mM stock solution and then cryopreserved at −70 °C. The collected control and experimental group cells were placed in a serum-free culture medium. Fluo-3/Am was added to a final concentration of 10 μM, and then incubated at 5% CO_2 in the dark for 30 min at 37 °C, with gentle shaking for several times during the incubation. Negative controls (without Fluo3-Am loading) were used for reference. The cells were observed and photographed by confocal microscopy (Nikon TE-2000-E, Japan).

Extracellular Ca^{2+} flux measurement

The microelectrode ion flux estimate (MIFE) technique was performed non-invasively to monitor the Ca^{2+} flux during apoptosis. Selective Ca^{2+} electrodes were used to measure the net Ca^{2+} flux in dense cell monolayers (Alavian *et al.* 2011, Valencia-Cruz *et al.* 2009). Briefly, 1 mL of the cell suspension sample (at a concentration of 1×10^5 cells/mL) was seeded in a petri dish. Cells in the logarithmic phase were treated with Pb^{2+}. Electrodes were calibrated in a range of Ca^{2+} standards before and after each experiment. Ion flux between two microelectrode positions – one close to the cell monolayer (5 μm) and one further away (up to 20 μm) – was measured as the electrochemical potential of Ca^{2+} at the two offset points.

Reactive oxygen species analysis

The 2′,7′-dichlorodihydrofluorescein diacetate (DCFH-DA, Molecular Probes, Eugene, OR) method was performed to evaluate the formation of reactive oxygen species (ROS). Cell concentrations were adjusted to $(1-2) \times 10^6$ cells/mL and loaded with 2′,7′-dichloro-diacetate (DCFH-DA, Molecular Probes, Eugene, OR) to a final concentration of 10 μM. Samples were incubated at 37 °C in 5% CO_2 for 20 min, gently shaken a few times, and then washed twice with serum-free medium to sufficiently remove intracellular DCFH-DA. Subsequently, the cells were observed and photographed using confocal microscopy (Nikon TE-2000-E, Japan).

Caspase-3, -8, and -9 activity assay

The activities of caspase-3, -8, and -9 were evaluated by using a colorimetric assay kit (Beyotime, Haimen City, Jiangsu Province, PR China). Protein concentrations of the supernatants of cell lysates (100 μL of lysate obtained from 2×10^6 cells) were determined using a Bradford assay kit (Beyotime). For each sample, 10 μL of supernatant was mixed with 10 μL of Ac-DEVDpNA (2 mM) for caspase-3, Ac-IETD-pNA (2 mM) for caspase-8, or Ac-LEHD-pNA (2 mM) for caspase-9 in assay buffer. Activity was determined with a spectrophotometer at 405 nm (ND-1000; NanoDrop Technologies, Wilmington, DE).

Reverse transcription-PCR (RT-PCR)

Total RNA of the cells was extracted, and the first complementary DNA (cDNA) chain was synthesized, according to the manufacturer's instructions using the PrimerScript™ RT kit (Takara, Dalian, China). Specific primer sequences of glyceraldehyde-3-phosphate dehydrogenase (GAPDH, a housekeeping gene), Bax, Bcl-2, Caspase-3, 8, Fas, and p53 were designed using Primer Premier 5.0 software (PREMIER BIOSOFT, Pa Palo Alto, CA), and synthesized by Shanghai Biological Technology Co. Ltd. (Shanghai, China). Optimal PCR conditions were as follows: 94 °C denaturation for 5 min, 32 cycles of 94 °C for 30 s, annealing at 72 °C for 30 s, and final extension at 72 °C for 12 min. PCR products were identified by 1.4% agarose gel electrophoresis.

Statistical analysis

We repeated each type of experiment at least three times and confirmed similar results. All values are presented as means ± SDs. Using the Statistical Analysis System (SAS Institute Inc., Cary, NC), the GLM data were analyzed and compared with a multiple comparison test (Duncan). $p < 0.05$ was considered statistically significant. $p < 0.01$ was considered highly statistically significant.

Results

Hoechst 33258 staining

Cells of the control group showed round or ovoid nuclei. The nuclear chromatin was uniformly stained, and they emitted strong fluorescence. The experimental group cells showed chromatin enrichment, nuclear pyknosis, uneven color, and bright spots. With the increase in lead acetate concentration, the cell nucleus changed significantly; some cells become crescent-shaped and they showed obvious dose-effect relationship (Figure 1(A)).

Transmission electron microscopy

The cells of the control group showed uniform cytoplasm. The nuclear double membrane structure was intact and the mitochondrial cristae were clearly observed. The nuclei were oval, with lightly stained nucleoli. Cells in the experimental group contained cytoplasmic vacuoles, but the double nuclear membrane structure was destroyed. Mitochondrial swelling was observed and the cristae had disappeared; only a partial cavity was observed. Cell chromatin appeared condensed and marginalized. The nuclear membrane showed cracks, with chromatin divided into blocks (Figure 1(B)).

Annexin V-FITC/PI double labeling

Annexin V-FITC/PI double marking combined with flow cytometry yielded a quantitative analysis of cell apoptosis.

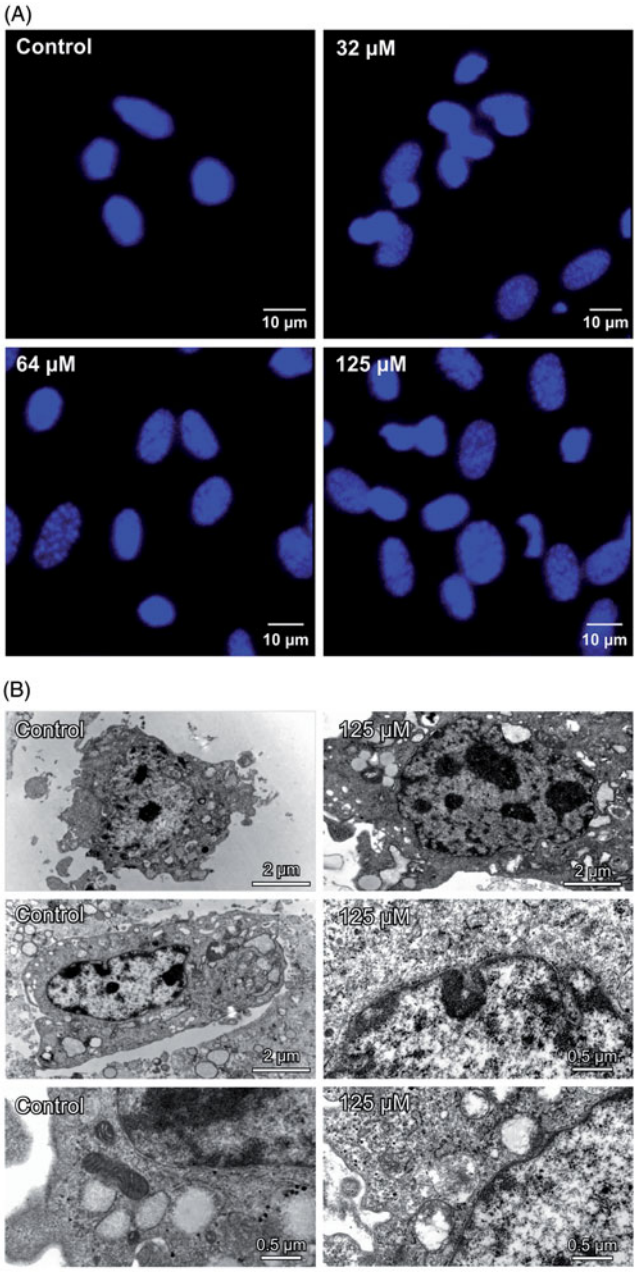

Figure 1. (A) Morphological observation of Siberian tiger fibroblast cells at 24 h after treatment with $Pb(Ac)_2$ using Hoechst 33258 staining by confocal microscopy. (B) Subcellular observation using transmission electron microscopy.

The results showed that when Siberian tiger fibroblasts were treated with 0 μM 32 μM, 64 μM, and 125 μM Pb^{2+}, at 12 h, 24 h, 36 h, and 48 h, respectively, the apoptosis rate increased from 0.4% to 9.7%. The increase in the apoptosis rate in the experimental group with the increase in Pb^{2+} concentration indicated that the apoptotic effect was dose- and time-dependent (Table 1).

Cell cycle analysis

PI staining was combined with flow cytometry to detect the changes in the cell cycle. The results of the treatment of Siberian tiger fibroblasts with 0 μM, 32 μM, 64 μM, and 125 μM Pb^{2+} for 24 h showed that the number of G0/G1 phase (the early stage of the DNA synthesis) cells was significantly increased while the number of S phase cells was decreased. This indicated an arrest in the G0/G1 phase, thereby inhibiting DNA synthesis. In the experimental group of the G2/M phase of DNA synthesis, the cell number first increased and then decreased compared to the control group (Table 2).

Table 1. Apoptosis rates (%) of Siberian tiger fibroblasts upon lead treatment ($\bar{X} \pm SD$, $n = 3$).

Group	12 h	24 h	36 h	48 h
Control	0.283 ± 0.076	0.533 ± 0.153	0.600 ± 0.200	1.867 ± 0.208
32 μM	0.413 ± 0.102	3.430 ± 0.252**	5.333 ± 0.451**	6.833 ± 0.321**
64 μM	0.473 ± 0.064	4.200 ± 0.436**	6.733 ± 0.351**	8.533 ± 0.379**
125 μM	1.060 ± 0.122*	6.733 ± 0.603**	8.967 ± 0.306**	9.667 ± 0.321**

Statistical significance to control is marked with (*) ($p < 0.05$) and (**) ($p < 0.01$).

Table 2. Cell cycle analysis of Siberian tiger fibroblasts treated with lead for 24 h ($\bar{X} \pm SD$, $n = 3$).

Phase	G0/G1(%)	S(%)	G2/M (%)
Control	38.24 ± 4.46	45.07 ± 4.59	9.57 ± 1.27
32 μM	46.76 ± 5.48*	33.25 ± 3.08*	16.50 ± 2.46**
64 μM	49.89 ± 5.67**	30.12 ± 3.39**	14.43 ± 1.88**
125 μM	56.70 ± 5.72**	36.35 ± 4.45	1.15 ± 0.08**

Statistical significance to control is marked with (*) ($p < 0.05$) and (**) ($p < 0.01$).

Mitochondrial membrane potential

JC-1 is a lipophilic cationic dye that can be selectively taken up into the mitochondria. Increase in membrane potential is indicated by the reversible change of color from green to red. In normal cells, JC-1 aggregates in the mitochondria and fluoresces red (FL3, 620 nm). In apoptotic or necrotic cells, JC-1 exists in the monomeric form and stains the cytoplasm green (FL1, 527 nm). Thus, the number of C gate cells reflects the mitochondrial membrane potential, and a greater number of C gate cells leads to a reduction in the mitochondrial membrane potential. After treatment with cadmium chloride, we observed a significantly decreased mitochondrial membrane potential compared with the control group ($p < 0.01$) (Figure 2).

Intracellular Ca^{2+} homeostasis

Fluo-3/AM is a new type of highly specific calcium fluorescent probe that reflects sensitive changes in the intracellular free Ca^{2+} concentration. In this study, Fluo-3/AM was used as a calcium fluorescent probe and apoptotic cells were observed under a confocal microscope. The results showed that increasing concentration of Pb^{2+} showed an increase in the proportion of the green fluorescent apoptotic cells and green fluorescence intensity, indicating that the concentration of free Ca^{2+} increased. In Pb^{2+} treatment groups (125 μM), green fluorescence was evenly distributed throughout the apoptotic cells, indicating that intracellular Ca^{2+} homeostasis had been severely affected (Figure 3(A)).

Extracellular Ca^{2+} flux measurement

Using real-time MIFE technique, extracellular Ca^{2+} flux before and after Siberian tiger fibroblast treatment with

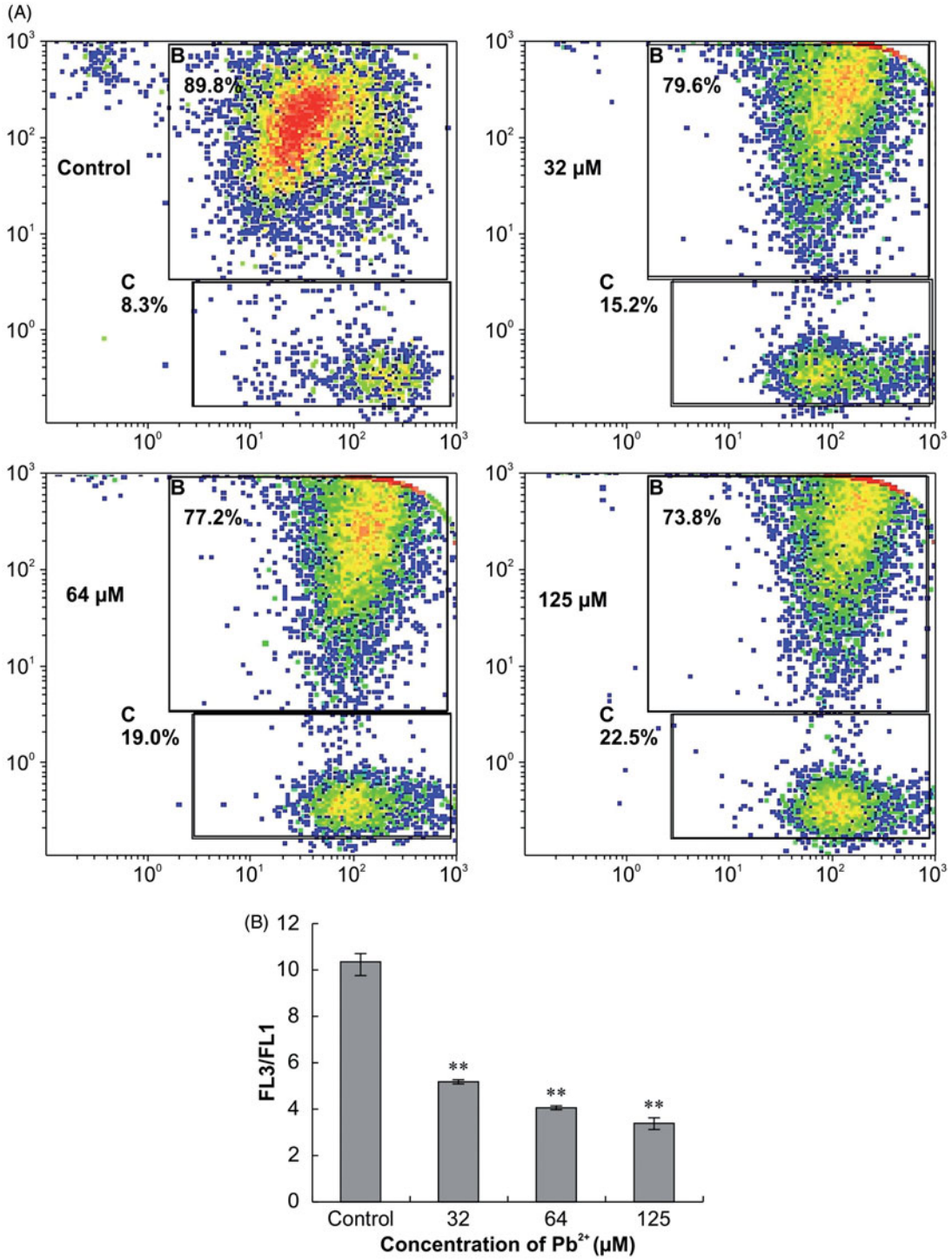

Figure 2. (A) and (B) Mitochondrial membrane potential of Siberian tiger fibroblast 24 h after treatment with lead. Statistically significant differences compared to the corresponding controls are marked with **($p < 0.01$) ($n = 3$).

125 μM Pb^{2+} was monitored. The recorded data is the Siberian tiger fibroblast extracellular calcium ion flow rate, which includes the size and direction of the flow of calcium ions (ordinate) and the abscissa record time. The zero line (positive) curve refers to Ca^{2+} ion efflux (Efflux), and the curve below the zero line refers to Ca^{2+} influx (Influx). The findings of our study suggest that Ca^{2+} dynamics was influx before Pb^{2+} treatment in cells (0–200 s); however, it became efflux after treatment with Pb^{2+} (200–800 s). The velocity magnitude increases compared with that before treatment. The difference was significant ($p < 0.01$), and the overall trend of velocity magnitude showed a decline (Figure 3(B)).

ROS analysis

DCFH-DA was used as a fluorescent probe for detecting ROS levels in apoptotic cells under a confocal microscope. With the increase in Pb^{2+} concentration, the number of green

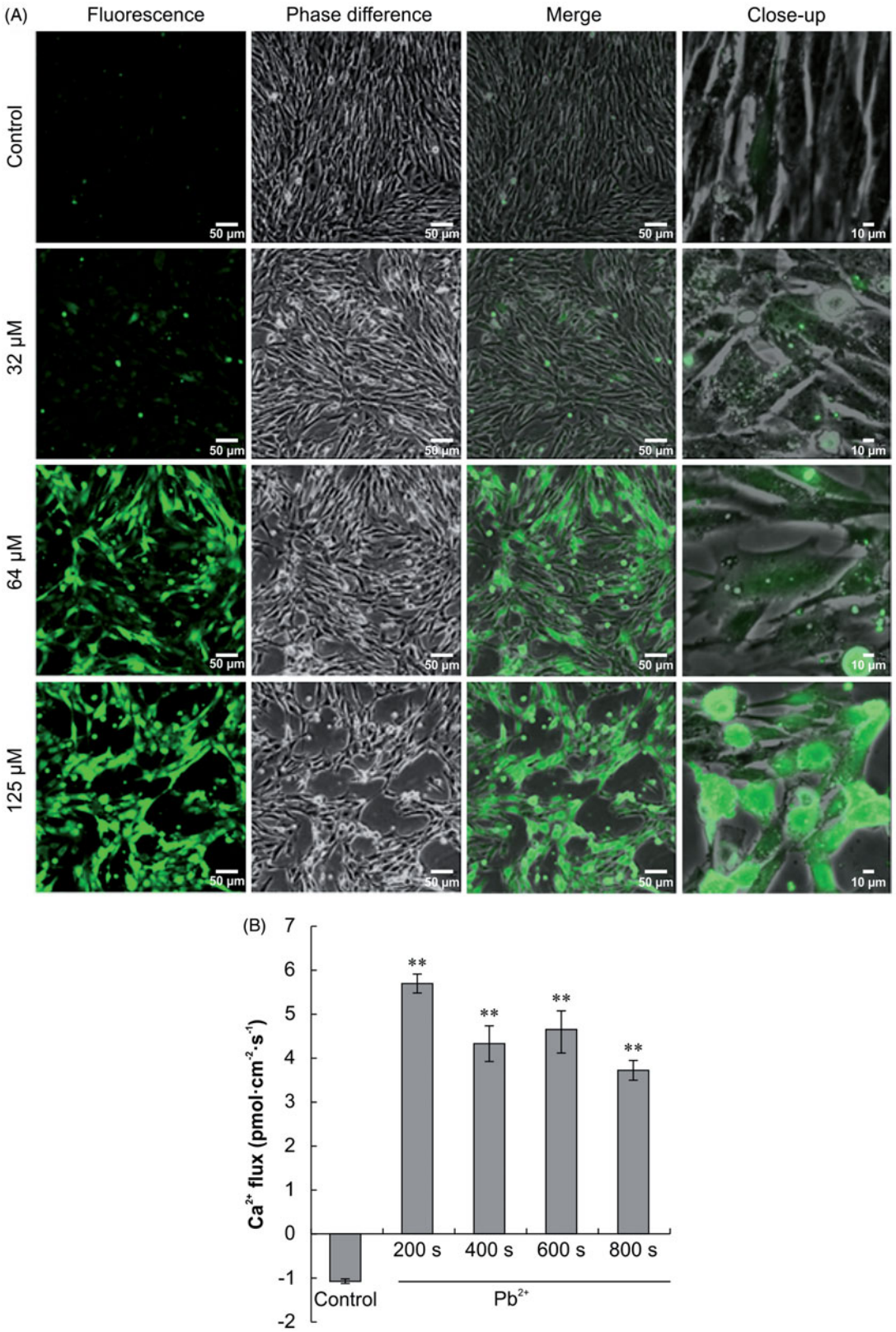

Figure 3. (A) Effects of Pb^{2+} on intracellular Ca^{2+} homoeostasis of Siberian tiger fibroblast treated for 24 h. Fluorescence, phase difference, and merge image scale bars are 50 μm. The close-up image scale bar is 10 μm. (B) Ca^{2+} flux in Siberian tiger fibroblast before and after treatment with 125 μM Pb^{2+}. Statistically significant differences compared to the corresponding controls are marked with ** ($p < 0.01$) ($n = 3$).

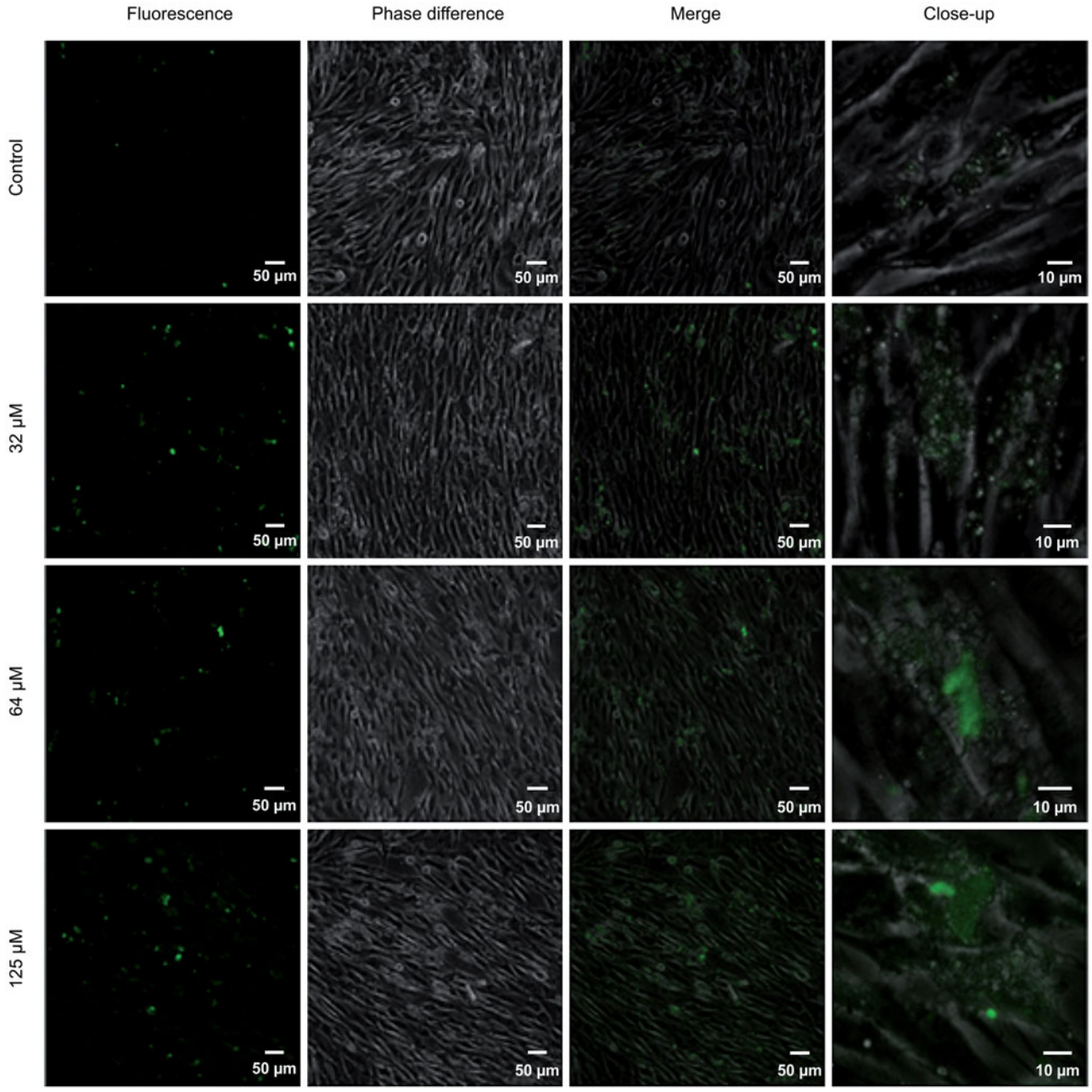

Figure 4. Effects of Pb^{2+} on Siberian tiger fibroblast intracellular ROS of were treated for 24 h. Fluorescence, phase difference, and merge image scale bars are 50 μm. The close-up image scale bar is 10 μm.

Table 3. Activities of caspase-3, -8, and -9 were determined in cytosolic extracts of Siberian tiger fibroblasts treated with lead for 24 h ($\bar{X} \pm SD$, $n = 3$).

Group	Caspase-3	Caspase-8	Caspase-9
Control	1.097 ± 0.007	1.176 ± 0.071	1.133 ± 0.060
32 μM	1.172 ± 0.087	1.400 ± 0.030*	1.441 ± 0.071*
64 μM	1.514 ± 0.047**	1.578 ± 0.078**	1.661 ± 0.055**
125 μM	1.685 ± 0.083**	1.893 ± 0.095**	1.913 ± 0.052**

Statistical significance to control is marked with (*) ($p < 0.05$) and (**) ($p < 0.01$).

fluorescent apoptotic cells increased. The proportion of green fluorescence intensity increased, indicating that ROS levels increased. A dose-dependent increase in ROS level was observed with increasing Pb^{2+} concentrations (Figure 4).

Caspase-3, -8, and -9 activity assays

We evaluated caspase-3, -8, and -9 activities by using a spectrophotometer to detect cleaved substrates; higher optical density $(OD)_{405}$ values reflect greater caspase activity. Caspase-3 activity was more pronounced in cells receiving 64 and 125 μM Pb^{2+} than in control cells ($p < 0.01$). Caspase-8 and -9 activities were significantly different in the 32 μM Pb^{2+} treatment group compared with the control group ($p < 0.05$), and the 64 and 125 μM Pb^{2+} treatment groups were also markedly high in caspase-8 and -9 activities compared with the control ($p < 0.01$, Table 3). These results indicate that Pb^{2+} activates caspase-3, -8, and -9 in Siberian tiger fibroblasts.

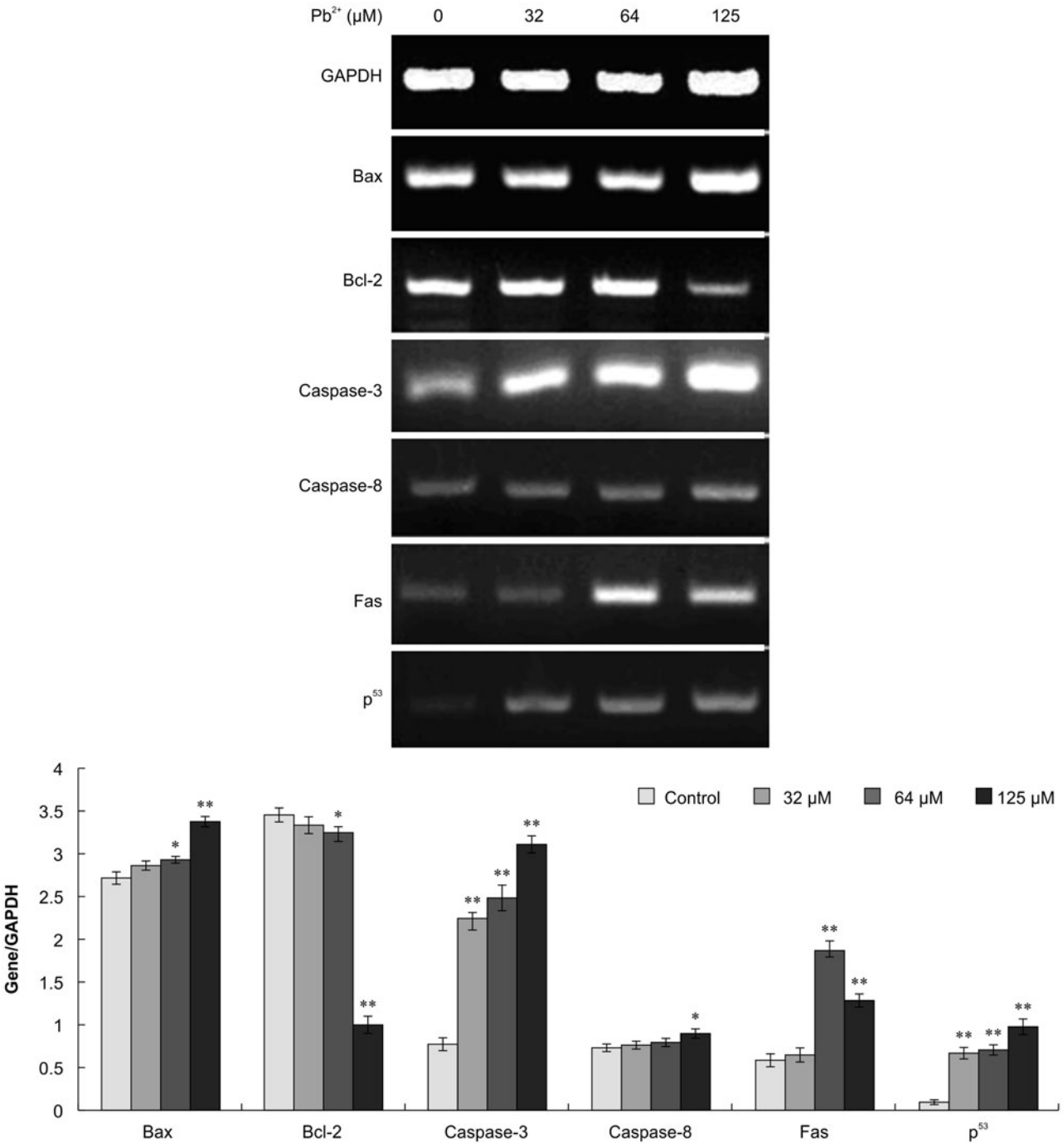

Figure 5. Analysis of Bax, Bcl-2, caspase-3, -8, Fas and p^{53} mRNA levels at 24 h (normalized to GAPDH). Statistically significant differences compared to the corresponding controls are marked with * ($p < 0.05$) and ** ($p < 0.01$) ($n = 3$).

RT-PCR

In this study, RT-PCR was performed to detect Bax, Bcl-2, caspase-3, caspase-8, Fas, and p53 expression levels of tiger fibroblasts that were treated with Pb^{2+}, with GAPDH as the reference gene. We observed that Bax, caspase-3, caspase-8, Fas, P53 gene expression increased with the increase in Pb^{2+} concentrations ($p < 0.05$ and $p < 0.01$, respectively). However, in the 125 μM treatment group, Fas gene expression was lower than that observed in the 64 μM treatment group. Bcl-2 gene expression decreased when the Pb^{2+} concentration increased. The Bax/Bcl-2 ratio showed an upward trend (Figure 5).

Discussion

Lead is an important heavy metal pollutant that has become widespread with the development of modern industries, and its hazardous effects in the living systems are increasing (Van Wijngaarden and Dosemeci 2006). It is being recognized as a major public health risk. Lead is a non-essential element in living organisms and can be found in water, soil, and air. Lead and its compounds can induce cell apoptosis and cause damage to multiple systems.

In this study, lead toxicity in Siberian tiger fibroblasts was studied. Lead was found to induce typical morphological changes, including subcellular structure destruction, cell

shrinking, and chromatin condensation. Lead also affects cellular function, for example, mitochondrial depolarization. Our study showed that the apoptotic effects were dose and time-dependent in the range of 0–125 μM Pb^{2+} and 12–48 h of exposure, respectively.

Physiological or pathological apoptotic stimuli are correlated with cell cycle progression (Kurochkin *et al.* 2011). In rat fibroblasts that were treated with Pb^{2+} for 48 h, cell cycle was arrested in the G0/G1 phase and a hypodiploid peak was observed (Iavicoli *et al.* 2001). Our data showed that Pb^{2+} exposure results in Siberian tiger fibroblast cycle arrest in the G0/G1 phase and inhibition of cell proliferation with decreased proportion of cells in the S phase. We confirmed that Pb^{2+} exposure caused fibroblast arrest in the G0/G1 phase (pre-DNA synthesis), thus interfering with cell proliferation and leading to apoptosis. This provides an important experimental basis for future studies on the mechanism of lead-induced apoptosis in Siberian tiger fibroblasts. In the experimental group, DNA synthesis and cell number in the G2/M phase of the DNA synthesis first increased and then decreased compared to the control group, probably because the proportion of cells in the G1 and S phase is large, resulting in reduced the proportion of cells in the G2 phase. Mitochondria have received unprecedented attention in research on apoptosis mechanisms because they play an important role in the regulation of the apoptotic process. The loss of mitochondrial membrane potential is a hallmark of apoptosis.

Studies have shown that lead binds to mitochondria at the ion-binding sites, leading to decreased membrane potential, thus transitioning the mitochondrial channel to the activated (open) state. Consequently, mitochondrial polarization, swelling, membrane rupture, and release of cytochrome C and other cytokines into the cytoplasm occur, resulting in apoptosis (Kulms and Schwarz 2002). This study showed that mitochondrial membrane potential in Siberian tiger fibroblasts shows a concentration-dependent decrease with lead exposure, thereby suggesting that lead-induced apoptosis of Siberian tiger fibroblasts is related to the mitochondrial apoptotic pathway. However, the sites of the toxic action of lead in mitochondria and the relative sensitivity of different mitochondrial processes to lead are not well understood.

Calcium as a second messenger plays an important role in apoptosis. Changes in the intracellular calcium ion concentration directly affect cell proliferation, differentiation, and apoptosis. Mobilization of calcium stores from the endoplasmic reticulum activates the apoptosis initiation factor as well as sensitizes mitochondria to direct proapoptotic stimuli.

Lead enters cells by calcium transport mechanisms, because lead has a similar coordination number as calcium due to an oxygen atom and a sulfur atom and its interacts more flexibly than calcium. Thus, lead competes with the calcium receptor, thereby affecting the intracellular second messenger activity. Since the affinity of lead to the calcium channel is much higher than that of calcium to the calcium channels, lead can replace the calcium-activated calcium channels, thereby leading to the activation of protein kinase. Protein kinases activate the cell membrane, endoplasmic reticulum, and mitochondrial calcium channel, such that intracellular Ca^{2+} influx from the endoplasmic reticulum and the mitochondria increases, leading to apoptosis (Orrenius *et al.* 2003). Our data demonstrated that cytosolic free Ca^{2+} levels increased when lead induced apoptosis of Siberian tiger fibroblasts, thereby disturbing the intracellular calcium homeostasis.

A study showed that lead can contribute to extracellular Ca^{2+} influx or efflux and inhibition of intracellular calcium ions. It can also lead to leakage of the Ca^{2+} from mitochondria or endoplasmic reticulum because of the accumulation of cytosolic Ca^{2+} in the cells (Yanamandra *et al.* 2011). However, our experimental results oppose those results. Our results of extracellular Ca^{2+} flux show that Ca^{2+} flux is influx before lead exposure and efflux after lead exposure. This result explains that intracellular free Ca^{2+} increases due to the release of endogenous calcium stores, rather than the absorption of extracellular calcium. Investigations on the role of interactions of Ca^{2+} in lead-induced apoptosis are important for understanding the mechanism of lead toxicity. Disturbed calcium homeostasis along with decrease in mitochondrial transmembrane potential presumably leads to endoplasmic reticulum calcium release.

Oxidative stress is a lead-induced apoptotic effect. Lead can promote the generation of ROS, reduce the concentration or activity of the antioxidants, and interfere with the oxidant-antioxidant balance, so that the body is in a state of oxidative stress (Chen *et al.* 2003). Lead can increase the neuronal activity of lipid peroxidation and inhibit the glutathione superoxide dismutase activity of neuronal cells from oxidative damage (El-Sokkary *et al.* 2003). Lead induces ROS generation *in vivo*, resulting in systematic mobilization and depletion of intrinsic antioxidant defenses and destabilization of calcium homeostasis by damaging electron transport. Consequently, ATP depletion, membrane ion channel disruption, leading to apoptosis is observed (Ercal *et al.* 1996). Our results show that lead can increase the levels of ROS in Siberian tiger fibroblasts, destroy the cell oxidation–antioxidation balance, resulting in oxidative damage. Presumably, lead-induced oxidative damage is one of the mechanisms underlying Siberian tiger fibroblast apoptosis.

The Bcl-2 gene family plays an important role in regulating apoptosis. Bcl-2 is an important apoptosis gene in the Bcl-2 gene family. Bax promotes apoptosis. When the Bax/Bcl-2 ratio increases, apoptosis increases, while apoptosis is inhibited when Bax/Bcl-2 ratio decreases (Yu *et al.* 2001).

During apoptosis, caspase-8 is activated, further activating caspase-9 and the most critical caspase-3 downstream. Caspase-3 is an important effector molecule for apoptosis execution. Most factors that trigger apoptosis eventually require caspase-3-mediated signal transduction pathways, leading to apoptosis. Our study found that lead significantly increases caspase-3 expression in a dose-dependent manner (Xu 2008). Our findings suggest that Pb^{2+}-induced apoptosis in Siberian tiger fibroblasts results from activation of caspase-3, -8, and -9, and thus, involves a caspase-dependent pathway.

Fas also plays a role in mediating apoptosis. Lead-induced Fas expression results in apoptosis (Friesen and Fulda 1997). Lead can induce cell apoptosis through multiple gene

pathways. The p53 gene is either wild-type or mutant. The wild type is involved in the process of apoptosis. Mutant P53 regulates gene expression of Bcl-2 and Bax; it inhibits the expression of Bcl-2, thereby promoting the expression of Bax to induce apoptosis (Fehsel *et al.* 1995).

Lead may induce PC12 cell apoptosis as it is associated with increased expression of p53, decreased expression of Bcl-2, and increased expression of Bax, thereby inducing apoptosis (Xu *et al.* 2006). Lead could significantly induce testicular germ cell apoptosis by increasing the gene expression of Fas in a dose-dependent manner (Dong *et al.* 2009).

Our results show that Bax, caspase-3, caspase-8, Fas, and p53 gene expression increases with increasing lead concentrations. The gene expression levels of Bcl-2 decrease with increasing lead concentrations; moreover, the gene expression of Bax/Bcl-2 ratio increases. Lead can affect the expression of several apoptosis-related genes in Siberian tiger fibroblasts.

Conclusions

In conclusion, lead induces apoptosis of Siberian tiger fibroblasts by blocking DNA synthesis, damaging mitochondrial function, interfering with calcium homeostasis, and causing oxidative damage and gene dysregulation. These results provide useful information for understanding the mechanisms of Pb-induced apoptosis of Siberian tiger fibroblasts and the adverse effects of Pb exposure in Siberian tigers. For the protection of Siberian tigers, fibroblasts as research material were used to understand the underlying mechanism of lead poisoning so that therapeutic strategies can be defined accordingly. However, the study was based on *in vitro* experimental systems, which do not fully reflect the mechanisms of Pb-induced apoptosis in Siberian tigers. We hope to perform further animal experiments of lead poisoning in Siberian tigers so that comprehensive experimental data is available to facilitate treatment of lead poisoning.

Disclosure statement

The authors have no competing interests to declare.

Funding

The work was supported by the Natural Science Foundation of Liaoning Province [2014022042], and the Agricultural Science and Technology Innovation Program (ASTIP) (cxgc-ias-01).

References

Alavian, K.N., *et al*., 2011. Bcl-xL regulates metabolic efficiency of neurons through interaction with the mitochondrial F_1F_O ATP synthase. *Nature Cell Biology*, 13, 1224–1234.

Ariza, M.E., and Williams, M.V., 1996. Mutagenesis of AS52 cells by low concentrations of lead(II) and mercury(II). *Environmental and Molecular Mutagenesis*, 27, 30–33.

Chen, L., Yang, X., and Jiao, H., 2003. Tea catechins protect against lead-induced ROS formation, mitochondrial dysfunction, and calcium dysregulation in PC12 cells. *Chemical Research in Toxicology*, 16, 1155–1161.

Dominguez, C., Solé, E., and Fortuny, A., 2002. In vitro lead-induced cell toxicity and cytoprotective activity of fetal calf serum in human fibroblasts. *Molecular and Cellular Biochemistry*, 237, 47–53.

Dong, S., *et al*., 2009. The role of MAPK and FAS death receptor pathways in testicular germ cell apoptosis induced by lead. *Acta Biochimica et Biophysica Sinica*, 4, 800–807.

Dong, S., Shan, Y., and Lu, M., 2005. Study on DNA damage and proliferation of testicular cells with lead exposed. *Chinese Journal of Public Health*, 21, 1216–1218.

El-Sokkary, G.H., Kamel, E.S., and Reiter, R.J., 2003. Prophylactic effect of melatonin in reducing lead induced neurotoxicity in the rat. *Cellular and Molecular Biology Letters*, 8, 461–470.

Ercal, N., *et al*., 1996. In vivo indices of oxidative stress in lead-exposed C57BL/6 mice are reduced by treatment with meso-2,3-dimercaptosuccinic acid or N-acetylcysteine. *Free Radical Biology &Amp; Medicine*, 21, 157–161.

Fehsel, K., *et al*., 1995. Nitric oxide induces apoptosis in mouse thymocytes. *Journal of Immunology*, 155, 2858–2865.

Friesen, C., and Fulda, S., 1997. Deficient activation of the CD 95(Apo1/Fas) system in drug resistant cells. *Leukemia*, 11, 1822–1841.

Gerber, G.B., Leonard, A., and Jacquet, P., 1980. Toxicity, mutagenicity and teratogenicity of lead. *Mutation Research*, 76, 115–141.

Goyer, R.A., 1993. Lead toxicity: current concerns. *Environmental Health Perspectives*, 100, 177–187.

IARC. 1987. Overall evaluation of carcinogenicity: an updating of IARC monographs. In IARC Monographs on the Evaluation of Carcinogenic Risks to Human, Vol. 1–42, Supplement 7. International Agency for Research on Cancer, Lyon, 230–232.

Iavicoli, I., Carelli, G., and Sgambato, A., 2001. Lead inhibits growth and induces apoptosis in normal rat fibroblasts. *Alternatives to Laboratory Animals: Atla*, 29, 461–469.

Kulms, D., and Schwarz, T., 2002. Independent contribution of three different pathways to ultraviolet-B-induced apoptosis. *Biochemical Pharmacology*, 64, 837–841.

Kurochkin, I.O., *et al*., 2011. Top-down control analysis of the cadmium effects on molluscan mitochondria and the mechanisms of cadmium-induced mitochondrial dysfunction. *American Journal of Physiology – Regulatory, Integrative and Comparative Physiology*, 300, R21–R31.

Kwong, W.T., Friello, P., and Semba, R.D., 2004. Interactions between iron deficiency and lead poisoning: epidemiology and pathogenesis. *The Science of the Total Environment*, 330, 21–37.

Matyushkin, E. N., *et al*., 1999. Distribution and numbers of Amur tigers in the Russian Far East in the mid-1990s. In: A.A. Aristova, ed. *Rare mammal species of Russia and neighboring territories (in Russian)*. Moscow: Russian Academy of Sciences Therological Society, 242–271.

Mielke, H.W., and Reagan, P.L., 1998. Soil is an important pathway of human lead exposure. *Environmental Health Perspectives*, 106, 217–229.

Miquelle, D. G., and Pikunov, D. G., 2003. Status of the Amur tiger and Far Eastern leopard. In: J.P. Newell, ed. *The Russian Far East: A Reference Guide for Conservation and Development*. McKinleyville, CA: Daniel and Daniel Publishers, 106–109.

Orrenius, S., Zhivotovsky, B., and Nicotera, P., 2003. Regulation of cell death: the calcium-apoptosis link. *Nature Reviews – Molecular Cell Biology*, 4, 552–565.

Roncal, C., *et al*., 2007. Lead, at low levels, accelerates arteriolopathy and tubulointerstitial injury in chronic kidney disease. *American Journal of Physiology – Renal Physiology*, 293, F1391–F1396.

Roy, N.K., and Rossman, T.G., 1992. Mutagenesis and comutagenesis by lead compounds. *Mutation Research*, 298, 97–103.

Russello, M.A., *et al*., 2004. Potential genetic consequences of a recent bottleneck in the Amur tiger of the Russian far-east. *Conservation Genetics*, 5, 707–713.

Srianujata, S., 1998. Lead- the toxic metal to stay with human. *The Journal of Toxicological Sciences*, 23, 237–240.

Valencia-Cruz, G., *et al*., 2009. Kbg and Kv1.3 channels mediate potassium efflux in the early phase of apoptosis in Jurkat T lymphocytes. *American Journal of Physiology – Cell Physiology*, 297, C1544–C1553.

Van Wijngaarden, E., and Dosemeci, M., 2006. Brain cancer mortality and potential occupational exposure to lead: findings from the national longitudinal mortality study, 1979–1989. *International Journal of Cancer*, 119, 1136–1144.

Villeda-Hernandez, J., *et al*., 2006. Morphometric analysis of brain lesions in rat fetuses prenatally exposed to low-level lead acetate: correlation with lipid peroxidation. *Histology and Histopathology*, 21, 609–617.

Xu, J., 2008. Study on the pathways of lead acetate-induced apoptosis in PC12 cells. Dissertation, Zhejiang University.

Xu, J., Ji, L.X., and Li, H., 2006. Lead-induced apoptosis in PC 12 cells: Involvement of p53, Bcl-2 family and caspase-3. *Toxicology Letters*, 166, 160–167.

Yanamandra, N., *et al*., 2011. Tipifarnib-induced apoptosis in acute myeloid leukemia and multiple myeloma cells depends on Ca^{2+} influx through plasma membrane Ca^{2+} channels. *The Journal of Pharmacology and Experimental Therapeutics*, 337, 636–643.

Yang, J.L., Yeh, S.C., and Chang, C.Y., 1996. Lead acetate mutagenicity and mutational spectrum in the hypoxanthine guanine phosphoribosyltransferase gene of Chinese hamster ovary K1 cells. *Molecular Carcinogenesis*, 17, 181–191.

Yin, F., and Huang, J.H., 1999. The status of the tiger and it's induced risk factors. *China Wildlife*, 20, 26–27.

Yu, X., Kubota, H., and Wang, R., 2001. Involvement of Bcl-2 family genes and Fas signaling system in primary and secondary male germ cell apoptosis induced by 2-bromopropane in rat. *Toxicology and Applied Pharmacology*, 174, 35–48.

Zelikoff, J.T., *et al*., 1988. Genetic toxicology of lead compounds. *Carcinogenesis*, 9, 1727–1732.